ANL-6534

Argonne National Laboratory

PHYSICS DIVISION

SUMMARY REPORT

April - May 1962

ANL-6534
Physics
AEC Research and
Development Report

ARGONNE NATIONAL LABORATORY
9700 South Cass Avenue
Argonne, Illinois

PHYSICS DIVISION SUMMARY REPORT

April-May 1962

Morton Hamermesh, Division Director

Preceding Summary Reports:

ANL-6455, November-December 1961
ANL-6488, January 1962
ANL-6517, February-March 1962

Operated by The University of Chicago

under

Contract W-31-109-eng-38

FOREWORD

The Summary Report of the Physics Division of the Argonne National Laboratory is issued monthly for the information of the members of the Division and a limited number of other persons interested in the progress of the work. Each active project reports about once in 3 months, on the average. Those not reported in a particular issue are listed separately in the Table of Contents with a reference to the last issue in which each appeared.

This is merely an informal progress report. The results and data therefore must be understood to be preliminary and tentative.

The issuance of these reports is not intended to constitute publication in any sense of the word. Final results either will be submitted for publication in regular professional journals or, in special cases, will be presented in ANL Topical Reports.

TABLE OF CONTENTS

The date of the last preceding report is indicated after the title of each project below. Projects that are not reported in this issue are listed on subsequent pages.

PAGE

PAGE

PROJECTS NOT REPORTED IN THIS ISSUE

A reference to the last preceding report is given in parentheses for each project.

I. EXPERIMENTAL NUCLEAR PHYSICS

I-7. Gamma-Ray Spectra from Capture in Neutron Resonances (ANL-6146, April-May 1960), L. M. Bollinger, R. T. Carpenter, and H. E. Jackson.

I-10. Tandem Van de Graaff Accelerator (ANL-6262, December 1960), F. P. Mooring and J. R. Wallace.

I-11. Installation and Operation of the Van de Graaff Generator (ANL-6488, January 1962), J. R. Wallace.

I-14. Pulsed Beams for the Van de Graaff Machine (ANL-6391, July-August 1961), R. E. Holland and F. J. Lynch.

I-18. Neutron Polarization and Differential Cross Sections (ANL-6517, February-March 1962), R. O. Lane and W. F. Miller.

I-28. Angular Correlations in Charged-Particle Reactions (ANL-6358, April-May 1961), T. H. Braid.

I-34. Decay of $_{68}Er^{172}$ (ANL-6432, September-October 1961), S. B. Burson and R. G. Helmer.

I-35. Decay of $_{57}La^{135}$ (19.5 hr) (ANL-6391, July-August 1961), S. B. Burson and H. A. Grench.

I-55. Capture Gamma-Ray Spectra for Neutrons with Energies from 0.1 to 10 eV (ANL-6052, September 1959), S. Raboy and C. C. Trail.

I-60. 7.7-Meter Bent-Crystal Spectrometer (ANL-6517, February-March 1962), R. K. Smither.

I-80. Molecular Beam Studies (ANL-6517, February-March 1962), L. S. Goodman, W. J. Childs, J. Dalman, and D. von Ehrenstein.

V-4. Relative β-Decay Probabilities for $_{19}K^{40}$ (ANL-6455, November-December 1961), D. Kurath.

V-8. Relationships of Collective Effects and the Shell Model (ANL-6358, April-May 1961), D. Kurath.

V-9. Interpretation of Experiments Involving Excitation of the 15.1-MeV Level of C^{12} (ANL-6391, July-August 1961), D. Kurath.

V-15. Statistical Properties of Nuclear Energy States (ANL-6488, January 1962), N. Rosenzweig.

V-25. Scattering of Alpha Particles by a Vibrational Nucleus (ANL-6517, February-March 1962), L. J. Tassie.

V-33. Flux Quantization and Time-Reversal Degeneracy (ANL-6517, February-March 1962), M. Peshkin and W. Tobocman.

V-42. Time Reversal and Superselection (ANL-6488, January 1962), H. Ekstein.

V-46. Elastic Nucleon-Nucleon Scattering at High Energies and Small Angles (ANL-6517, February-March 1962), K. Hiida.

I. EXPERIMENTAL NUCLEAR PHYSICS

I-2-20 Neutron Detectors (51210-01)

S. I. Baker, L. M. Bollinger, and G. E. Thomas
Reported by G. E. Thomas

A STUDY OF RESOLUTION WIDTHS OF BORON-CONTAINING AND LITHIUM-CONTAINING GLASS SCINTILLATORS

In the initial measurements taken for the paper by Bollinger et al.[1] to determine the pulse heights and resolutions for thermal neutrons for various glasses, care was used to provide a long pulse-integrating time in the circuitry, a good reflector, and a photomultiplier that had a narrow pulse-height distribution with a NaI(Tl) scintillator. Even with these precautions, the resolution width for our lithium glass GL-304[2] was repeatedly measured to be in the range of 15-20% and was frustratingly irreproducible. As a final effort, it was decided to use a photomultiplier, if available, that had a very uniform photocathode sensitivity. For this we used the "standard tube" made available by the Argonne Electronics Division.

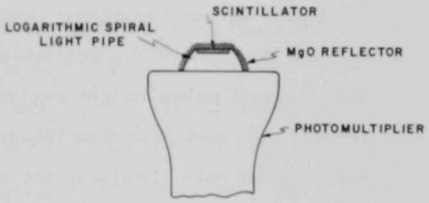

Fig. 1. Scale drawing of the optical system used in the final measurements of pulse-height distributions. The scintillators are 2.0 cm in diameter and 0.23 cm thick. The logarithmic-spiral light pipe is made of lucite. The photomultiplier is the special DuMont type 6363 tube described in the text.

The experimental arrangement is that shown in Fig. 1. This "standard tube" is a DuMont 6363 that has been set aside for

[1] L. M. Bollinger, R. J. Ginther, and G. E. Thomas (submitted to Nuclear Instr. and Methods).

[2] Glass supplied by R. J. Ginther of N.R.L. Composition given in reference 1.

reference purposes. In the area covered by our glass scintillators (2.0 cm diameter) the sensitivity of the photocathode varies by less than ± 6%. This exceptionally good photomultiplier has a luminous efficiency of 91 μA/lu and gives a resolution width (full width at half maximum divided by mean pulse height) of 8.9% when the light intensity per pulse from a pulsed light source is 100/661 of the intensity given by a 661-keV gamma ray in a NaI(Tl) scintillator mounted on the logarithmic-spiral[3] light pipe of Fig. 1. This special light pipe was designed to collect nearly all of the available light. Each sample was cut to exactly the same size (0.23 cm. thick × 2.0 cm. diameter) and the photomultiplier, light pipe, and scintillator were coupled together with silicone grease. MgO was carefully packed around the light pipe and on top of the scintillator to ensure collection of as large a fraction of the available light as possible. A conventional 256-channel pulse-height analyzer was used with long time constants throughout, and care was taken that the peak of the thermal neutron distribution was always in the same channel for each sample. The same high voltage and amplifier gain were used throughout. The gain was varied by an attenuator which had an error of less than 1% over the region used. The slow-neutron source used was 1 g of Po-Be with a graphite moderator and a 2-in. lead filter.

It was discovered that the optical properties of the system play a significant role in determining the numerical values of pulse heights. Two different qualitative effects need to be considered. First, a nonuniformity in the sensitivity of the photocathode was found to be surprisingly important—presumably because the geometrical conditions for light collection are not the same for different modes of excitation of a scintillator nor for different scintillators. Second, the fraction

---

[3] W. C. Kaiser, A. J. MacKay, and W. W. Managan, Argonne National Laboratory Report ANL-6196 (1960).

of the emitted light that is extracted from a scintillator was found to depend on the optical properties of the system, an important effect since the fraction extracted also depends on the index of refraction of the scintillator. In particular, for a glass scintillator having approximately the same index of refraction as the glass of the photomultiplier and as the grease used as a coupling agent, the light escapes with great ease in comparison with the light from NaI(Tl), for which a high index of refraction encourages total internal reflection. As a result, special care is required if a precise and meaningful comparison is to be made between the pulse heights of a glass scintillator and a reference scintillator such as NaI.

Both of the optical difficulties encountered with the scintillators mounted directly on the photomultiplier were largely eliminated by using the optical system shown in Fig. 1. The key element in the system is the light pipe, shaped in a special form of the logarithmic spiral.[3] Recessing the scintillator into the light pipe maximizes the probability that the light will escape from the scintillator, thus minimizing the influence of the index of refraction. Furthermore, the light pipe tends to distribute the light uniformly over the surface of the photocathode, independent of the point of emission, thus minimizing the effects resulting from nonuniformity of the cathode.

An example of a pulse-height distribution resulting from excitation of a boron-containing glass by slow neutrons is given in Fig. 2. The peak on the right is formed by the charged particles from the reaction $B^{10}(n,\alpha)Li^{7}$ and the rise in counting rate near zero pulse height is caused by photomultiplier noise and, for some scintillators, by a long-term luminescence of the glass. Figure 3 gives the corresponding distribution for the $Li^{6}(n,\alpha)T$ reaction in a lithium

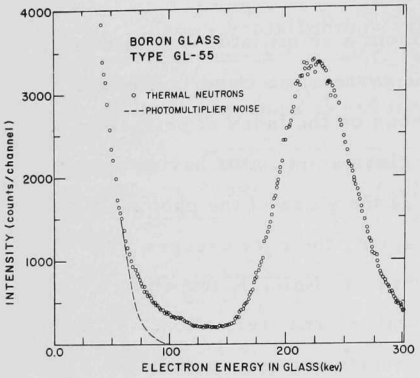

Fig. 2. Pulse-height distribution of the boron-glass scintillator GL-55, when excited by thermal neutrons. The pulse-height scale (abscissa) is the electron energy that would be required to give a pulse of the indicated height.

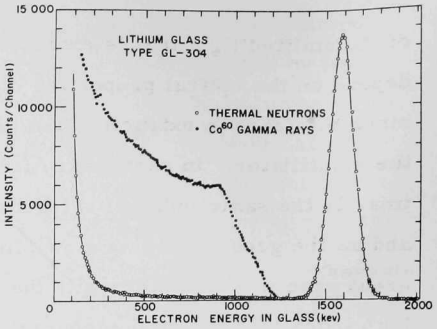

Fig. 3. Pulse-height distribution of the lithium-glass scintillator GL-304 for excitation by Co^{60} gamma rays and by thermal neutrons. The abscissa is the electron energy required to give a pulse of the indicated height.

glass. In addition, the pulse-height distribution for Co^{60} gamma rays (1.17 and 1.33 MeV) is given in Fig. 3.

The results of the measurements of pulse heights are summarized in Table I. The equivalent energy E_x expended in the NaI is calculated from the relation $E_x = (661\ \text{keV})\beta$, where β is the ratio of the height of the pulse being considered to the height of the pulse from a 661-keV gamma ray on NaI(Tl). It should be noted that our NaI equivalent values are somewhat lower than those reported by others. This is probably the result of collecting more nearly all of the available light from the NaI when using this logarithmic-spiral light pipe. Our resolution width of 9.5% for the lithium glass GL-304 is seen to be very much narrower than the width of 18% obtained by Firk et al.[4] for the same

[4] F. W. Firk, G. G. Slaughter, and R. J. Ginther, Nuclear Instr. and Methods 13, 313 (1961).

TABLE I. Pulse heights of glass scintillators.

Glass number[a]	100 R_1[b]	100 R_2[b]	Equivalent electron energy of neutron pulses		Resolution width for neutron pulses (%)
			Glass (keV)	NaI (keV)	
Boron glasses					
GL-127	12.0	5.3	272	14.4	23
GL-707	9.0	4.0	206	8.3	30
GL-55	9.1	3.6	208	7.4	33
Lithium glasses					
GL-231	34	7.6	1630	124	8.85
GL-304	33	6.1	1590	97	9.5

[a] The composition of the various glasses is given in reference 1.

[b] $R_1 = \frac{\text{p.h. for neutrons in glass}}{\text{p.h. for equal dissipation of energy by electrons in glass}}$

$R_2 = \frac{\text{p.h. for electrons in the glass}}{\text{p.h. for electrons of the same energy in NaI(Tl)}}$

kind of glass or than the width of about 20% calculated from the curves given by Anderson et al.[5] Moreover, the width of 23% for the boron glass GL-127 is much narrower than the width of 45% previously reported by us.[6]

[5] D. G. Anderson, J. Dracass, and P. Flanagan, in Instruments and Measurements, edited by H. von Koch and G. Ljungberg (Academic Press, New York and London, 1961), Vol. 2, p. 616.

[6] L. M. Bollinger, G. E. Thomas, and R. J. Ginther, Rev. Sci. Instr. 30, 1135 (1959).

The major step required to reduce the resolution widths to the values given in Table I was to use the "standard tube" photomultiplier described above. Even for this special tube, however, nonuniformity of the cathode appears to broaden the resolution significantly since the pulse-height distribution for neutrons is improved somewhat by using a light pipe. For example, the resolution width of the lithium glass GL-304 is 10.2% when the scintillator is mounted directly on the photomultiplier and drops to 9.5% when the logarithmic-spiral light pipe of Fig. 1 is used.

That nonuniformity of the photocathode is an important source of resolution broadening for most photomultipliers is confirmed by our experience with a tube having a typical degree of nonuniformity. This tube exhibited a good resolution for NaI (7.5% for Cs^{137}) but a poor resolution (about 20%) for the lithium glass GL-304 when the glass was mounted directly on the photocathode. However, when this same scintillator and photomultiplier were coupled together by means of a cylindrical light pipe 2 cm long the resolution width dropped to 13%. Apparently this difference results from the light pipe providing a more uniform illumination of the photocathode. The unusually great sensitivity of the glass scintillators to a nonuniformity of the photocathode probably is due to the near equality of the refractive indices of the glass scintillator, the optical grease, and the glass of the photomultipliers. As a result, the emitted light is able to escape from the scintillator with very few reflections. This tends to make the height of a given pulse strongly dependent on the local sensitivity of the photocathode. The above discussion and data suggest that nonuniformity of the photocathode plays a much more important role than is generally recognized in determining the resolution width for other kinds of scintillators and, in particular, for the organic scintillators used as energy spectrometers for fast neutrons.

I-3-21 Cross-Section Measurements with the Fast Neutron Velocity Selector (51210-01)

L. M. Bollinger, L. M. Bogan, R. T. Carpenter, R. E. Cote', H. E. Jackson, J. P. Marion, and G. E. Thomas
Reported by H. E. Jackson

TOTAL CROSS SECTION OF MOLYBDENUM

We are currently studying the resonant-capture γ-ray spectra of molybdenum in two experiments in which the time-of-flight resolution is moderately poor (approximately 80 nsec/m). This disadvantage is normally overcome by analyzing data in the light of the known high-resolution transmission data. However, only measurements of relatively poor quality,[1] made before 1956, are available in the case of molybdenum. For this reason we have made a preliminary measurement of the total cross section of molybdenum, with the main purpose of locating and determining the relative strengths of neutron resonances under conditions of improved resolution.

The neutron transmissions of samples ranging from 0.317 to 1.270 cm in thickness were determined from measurements made with the Argonne fast chopper operated with a time-of-flight resolution of approximately 30 nsec/m. The cross section as a function of energy is shown in Fig. 4. The resonance at 12 eV was previously undetected as were twelve other resonances evident in the new results in the region below 400 eV. Analysis of the resonance at 12 eV gives a radiation width $\Gamma_\gamma = 0.110 \pm 0.010$ eV, and a neutron width $\Gamma_n = (0.019 \pm 0.004) \times 10^{-3}$ eV/ag, where a is the isotopic abundance of the nuclide in which capture occurs and g is the statistical factor. The capture γ-ray spectrum (obtained by summing the heights of coincident pulses from two crystals)[2] for the 12-eV resonance was

---

[1] Brookhaven National Laboratory Report BNL-325.

[2] H. E. Jackson and L. M. Bollinger, Phys. Rev. 124, 1142 (1961).

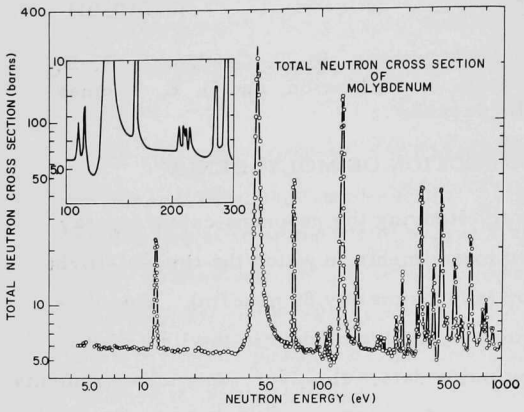

Fig. 4. Measured total neutron cross section of molybdenum.

measured in an attempt to make an isotopic assignment. The high-energy cutoff indicates a neutron binding energy of 5.9 ± 0.1 MeV for the capturing nuclide. Lacking knowledge of the precise values of the binding energies of even nuclides, we were only able to limit possibilities to Mo^{98} or Mo^{100}. A compilation of the measured cross sections has been submitted to the BNL Cross-Section Evaluation Center.

I-19-10 Nuclear Resonance Absorption of Gamma Rays (51210-01)

S. S. Hanna, G. J. Perlow, J. P. Schiffer, and J. A. Weinman
Reported by J. P. Schiffer

SEARCH FOR AN EFFECT OF MAGNETIC FIELDS ON ELECTROMAGNETIC RADIATION

Accepted electromagnetic theory does not predict any change in frequency for radiation passing through a magnetic field. However, some scattering effects are expected to take place at very high magnetic field strengths.[1] For example, it has been suggested that

---

1 Julian Schwinger, Phys. Rev. 82, 664 (1950).

some anomalies in astronomical observations may involve a photon-photon interaction of the type

$$\frac{\Delta \nu}{\nu} = K \ell u,$$

where K is a constant equal to 2.6×10^{-15}, ℓ is the path length in cm, and u is the energy density in erg/cc.[2] It has been suggested that the Mössbauer effect might be used to provide a test of this hypothesis if the radiation could be passed through a region of high photon density such as might be obtained in the vicinity of plasma.[3] Since this form of this proposed interaction does not contain any frequency dependence and since if it were to exist it would contradict accepted electromagnetic theory, it seemed that assuming u to be the energy density due to any electromagnetic field was not an unallowable extension of an already radical hypothesis. It is true that a static magnetic field does not contain photons and therefore this experiment does not fully test the hypothesis stated in Eq. (1). However, a magnetic field produces by far the largest electromagnetic energy density obtainable in the laboratory[4] and thus provides a conveniently easy experiment.

The measurements were carried out by allowing the 14-keV gamma rays emitted by Fe^{57} to pass through transverse and longitudinal magnetic fields produced by permanent magnets. The velocity spectrometer used will be described elsewhere.[5] The source used was

---

[2] E. Finnlay-Freundlich, Phil. Mag. 45, 303 (1954); M. Born, Proc. Phys. Soc. (London) A67, 193 (1954).

[3] A. Ward, Nature 192, 858 (1961).

[4] This was pointed out to us by J. Heberle.

[5] G. J. Perlow (to be published).

Co^{57} diffused into Cu. The absorber was $Na_4Fe(CN)_6 \cdot 10H_2O$ with the Fe enriched in Fe^{57}. This combination produced a single absorption line approximately 45% deep (without background corrections) and 0.5 mm/sec wide.

In the gap traversed by the gamma radiation, the magnetic field was 5500 oersted at the center and fell off to half this value in about 0.5 in. from the center. From Eq. (1), this would give a frequency shift of about 5×10^{-9}. We have also made a measurement with the magnetic field along the direction of the photons. This was done by providing a horseshoe magnet with pole pieces pierced by a 0.75-in. hole. This allowed radiation to go through one pole piece, cross the gap in a direction parallel to the magnetic field, and emerge through the hole in the other pole piece. The field in the gap of this magnet was 1700 oersted and the calculated effect was about 5×10^{-10}. Along this longitudinal path, the magnetic field in the gap was in the direction of propagation of the gamma photons but was oppositely directed outside the magnet. Hence the line integral of the field along the path was zero. To allow for the possibility of a directional effect, the experiment was also repeated with the source placed in the field-free region inside the hole in the pole tip. The effect calculated from Eq. (1) in this case was 5×10^{-11}.

The data obtained from the velocity spectrometer were analyzed by a least-squares program. The principal source of error in the measurement was from counting statistics. This error was doubled to allow for systematic errors such as temperature fluctuations within the instrument. The results are shown in Table II below. It is clear there is no effect of a magnitude comparable to the one expected from Eq. (1). This is not at all surprising. The interpretation of the evidence supporting Eq. (1) has been seriously questioned by several authors,[6] one of whom

---

[6] W. H. McCrea, Phil. Mag. 45, 1010 (1954); F. M. Burbidge and G. R. Burbidge, Phil. Mag. 45, 1019 (1954); D. ter Haar, Phil. Mag. 45, 1023 (1954); L. Helfer, Phys. Rev. 96, 224L (1954).

TABLE II. Summary of results.

Type of field	Measured effect $\left(\frac{\Delta\nu}{\nu}\right)$	Effect calculated from Eq. (1)
Transverse	$(2 \pm 4) \times 10^{-15}$	-5×10^{-9}
Longitudinal $\left(\int \vec{B} \cdot \vec{ds} = 0\right)$	$(1 \pm 5) \times 10^{-15}$	-5×10^{-10}
Longitudinal $\left(\int \vec{B} \cdot \vec{ds} \neq 0\right)$	$(1 \pm 4) \times 10^{-15}$	-5×10^{-11}

suggested that such an effect might be present but that K should be only a thousandth of the value given above.[7] It is clear that we have not observed even this diminished effect. It must also be made clear that our measurement does not really constitute a test of Eq. (1) anyway since this experiment used static magnetic fields which do not contain photons. On the other hand, to our knowledge there have been no previous measurements in which the influence of magnetic fields on the frequency of photons has been tested to such accuracy. Our results can stand on this ground alone, without reference to any theoretical expectation. The experiment could be repeated with at least 10-fold greater accuracy by using techniques developed for measuring the gravitational red shift. Further increase in accuracy could be obtained by the use of electromagnets which can produce considerably stronger magnetic fields. We are indebted to Dr. M. R. Perlow for preparing the enriched absorber.

[7] M. A. Melvin, Phys. Rev. 98, 884 (1955).

I-22-17 Scattering of Charged Particles (51210-01)

J. L. Yntema

I. INTRODUCTION

Angular distributions and absolute cross sections have been measured for the triton groups observed in the (d, t) reaction on enriched metallic targets of Ti^{46}, Ti^{47}, Ti^{48}, Ti^{49}, and Ti^{50} at a deuteron energy of 21.4 MeV. The results are compared with pickup reactions on other targets in this region of the periodic table and with the results from (d, p) and (d, d) reactions on the titanium isotopes.

II. EXPERIMENTAL PROCEDURE

The experiment was performed with the 21.4-MeV deuteron beam of the 60-in. cyclotron bombarding targets in the Argonne 60-in. scattering chamber.[1] The experimental techniques have been described elsewhere. In the present experiment the detector system was different from the one used previously. The NaI crystal which was used as the dE/dx detector was placed at a 45° angle in front of the photomultiplier which views it through an air light pipe. The improved light collection permitted a reduction in the thickness of the crystal without loss of resolution in the particle-identification system. The new arrangement permits the use of either a NaI crystal or a silicon detector as the E detector and extends the energy range of the triton spectra to lower energies.

The target material was obtained as enriched TiO_2 from Oak Ridge National Laboratory. It was reduced by means of the iodide process[2] to titanium metal which was subsequently rolled to a thickness of approximately 1 mg/cm^2.

---

[1] J. L. Yntema and H. W. Ostrander, Nuclear Instr. and Methods (to be published).

[2] This work was done at Battelle Memorial Institute, Columbus, Ohio.

Since a possibility of calcium contamination was introduced in the reduction process, both the spectrum and the angular distribution of the $Ca^{40}(d, t)Ca^{39}$ reaction were measured in order to check on this possibility. Furthermore, it is possible that some Ta may have diffused from the Ta core wire on which the Ti metal was deposited. However in the present experiment the effects of Ta impurities were found to be completely negligible, if present at all.

The energy calibration was obtained from the range-energy relation as well as from the Q values of known reactions. In general, the calibration is accurate to about 100 keV over the entire range. The relative cross sections are reliable within the statistical errors except for those peaks where an appreciable contribution from other isotopes of Ti had to be subtracted. The absolute cross sections of the main peaks are reliable within less than 10%.

Energy spectra were obtained in 3° intervals from 12° to 36°. This angular range is sufficient to identify $\ell = 1$, $\ell = 2$, and $\ell = 3$ transitions.

III. EXPERIMENTAL RESULTS

The results are tabulated in Table III. The table gives the energies of the groups with either $\ell = 3$ or $\ell = 1$ transitions, together with their absolute differential cross sections measured at 21° for $\ell = 3$ transitions and at 27° (the approximate location of the second maximum) for $\ell = 1$ transitions. The last column lists the number of $f_{7/2}$ neutrons involved in the transitions. This number was obtained by assuming that the combined cross sections for the two $\ell = 3$ transitions observed in Ti^{50} correspond to 7.2 $f_{7/2}$ neutrons. This value was chosen as a reasonable estimate of the number of particles when account was taken of the admixture of 2p neutrons and the probability that some of the cross sections would proceed to the higher isobaric-spin states[3] which could

[3] J. B. French and M. H. Macfarlane, Nuclear Phys. 26, 168 (1961).

TABLE III. Cross sections for strong groups.

Final nucleus	Exc. energy	$d\sigma/d\omega$ at 21° c.m.	$d\sigma/d\omega$ at 27° c.m.	Number of particles
Ti^{45}	0	2.58		1.83
	0.37			
	1.74	1.42		1.08
	3.1			
Ti^{46}	0.88	0.95		0.67
	2.07	1.25		0.89
	3.30	0.17		0.12
	3.94	1.94		1.38
	4.40	0.85		0.60
	5.84	0.60		0.43
Ti^{47}	0.16	3.32		2.26
	1.6		0.39	
	2.47	2.08		1.48
Ti^{48}	0	0.44		0.31
	0.98	1.20		0.85
	2.33	0.85		0.60
	3.30	3.27		2.32
	4.60			
	4.90	1.85		1.31
	5.60	0.72		0.51
	6.20	0.81		0.58
Ti^{49}	0	5.91		4.20
	1.45		0.47	
	2.52	4.26		3.02

not be observed in the present experiment. The normalization process used does not take account of the dependence of reduced width on Q, nor does it take account of variations of the optical-model potentials between isotopes. Preliminary results on the elastic deuteron scattering indicate that there are differences between the diffraction patterns for different isotopes and that these show a systematic trend with neutron excess and are not explained by a change in the interaction radius. The number of particles given in Table III should, therefore, be treated as a rather tentative quantity.

A. The $Ti^{50}(d, t)Ti^{49}$ Reaction

The spectrum at 21° lab is shown in Fig. 5. The strong peaks to the ground state and to the states near 2.5 MeV have an $\ell = 3$ angular distribution, while the group proceeding to states near 1.5 MeV has an $\ell = 1$ angular distribution. Since Ti^{50} has 28 neutrons, the ground-state configuration is expected to be mainly a closed $f_{7/2}$ neutron shell. From the presence of the $\ell = 1$ transition to states near 1.5 MeV, it follows that there is some 2p neutron admixture in the ground state. A similar admixture of 2p protons in the ground-state wave function, which should have a closed $1f_{7/2}$ proton shell, has been observed in

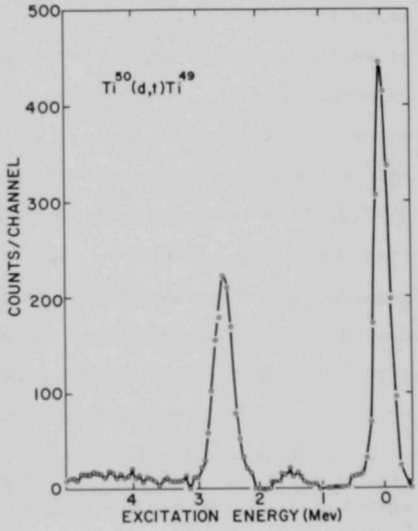

Fig. 5. The spectrum of $Ti^{50}(d, t)Ti^{49}$ at 21° lab. The spectrum has been corrected for the contributions from the Ti^{49} and Ti^{48} contained in the Ti^{50} target.

the $Ni^{58}(d, He^3)Co^{57}$ reaction.[4] However, strong $\ell = 1$ transitions have not been observed in other nuclei with 28 neutrons.[5-8]

The neutron ground-state configuration of Ti^{49} is expected to be mainly $(1f_{7/2})^{-1}$. Thus if one assumes that the neutrons and protons do not interact, or alternatively that the neutron-proton eigenfunctions for particles in the $1f_{7/2}$ shell have well-defined seniority, the $Ti^{50}(d, t)Ti^{49}$ and $Ti^{48}(d, p)Ti^{49}$ reaction should proceed only to the ground state of Ti^{49}. On the basis of this assumption, Schiffer et al.,[9] in their (d, p) experiment on natural titanium, identified the $\ell = 3$ transition observed at 2.5 MeV in the gross-structure spectrum as the $f_{5/2}$ single-particle state. If this assignment were correct, Ti^{50} would contain a very large admixture of $1f_{5/2}$ neutrons in its ground-state configuration. Such an admixture would appear to be unlikely in view of the relatively small admixtures of $1f_{5/2}$ neutrons in targets with 30 and 32 neutrons. Furthermore, the fact that the ratio of the intensity of the 2.5-MeV transition to that of the ground-state transition are the same in $Ti^{50}(d, t)Ti^{49}$ and in $Ti^{48}(d, p)Ti^{49}$ strongly indicates that the 2.5-MeV transition involves the transfer of a $1f_{7/2}$ neutron. This indicates that only about 58% of the ground-state eigenfunction has seniority 1 and that the remaining 42% is distributed between the $J = \frac{7}{2}$ states at about 2.5 MeV excitation. States with nondefinite seniority have already been used to calculate some

---

[4] J. L. Yntema, T. H. Braid, B. Zeidman, and H. W. Broek, Proceedings of the Rutherford Jubilee International Conference, Manchester, 1961, edited by J. B. Birks (Heywood and Co. Ltd., London, 1961), p. 521.

[5] B. Zeidman, J. L. Yntema, and B. J. Raz, Phys. Rev. 120, 1723 (1960).

[6] M. H. Macfarlane, B. J. Raz, J. L. Yntema, and B. Zeidman, Phys. Rev. (to be published).

[7] C. D. Goodman, J. B. Ball, and C. B. Fulmer, Phys. Rev. (to be published).

[8] A. G. Blair and H. E. Wegner (to be published).

[9] J. P. Schiffer, L. L. Lee, Jr., and B. Zeidman, Phys. Rev. 115, 427 (1959).

properties of nuclei in the $1f_{7/2}$ shell.[10] Lawson and Zeidman[11] have found that the eigenfunctions used in reference 10 can also explain the transition strengths obtained in the (d,t) experiment. Similar effects have been observed in other nuclei with 28 neutrons. In the $Fe^{54}(He^3,\alpha)Fe^{53}$ reaction,[8] three peaks with $\ell = 3$ angular distributions were observed.

A number of states in Ti^{49} have been observed in the $Ti^{48}(d,p)Ti^{49}$ reaction in the region in which the $\ell = 1$ transition is observed in the $Ti^{50}(d,t)Ti^{49}$ reaction. In their $Ti^{48}(d,p)Ti^{49}$ experiment, Rietjens et al.[12] observed strong $\ell = 1$ transitions to states at 1.38 and 1.72 MeV. The spins of these states have been shown to be $\frac{3}{2}^-$ and $\frac{1}{2}^-$, respectively.[13] The resolution in the present experiment is not good enough to separate these two states. However, the intensity of excitation of the 1.72-MeV state is estimated to be less than 30% of the intensity of the transition to the $\frac{3}{2}^-$ state.

It is possible to obtain an estimate of the admixture of p-shell particles if one uses the approach of Macfarlane et al.[6] This indicates that the admixture of 2p neutrons is approximately 0.4 ± 0.2 particles.

B. The $Ti^{49}(d,t)Ti^{48}$ Reaction

The spectrum from the $Ti^{49}(d,t)Ti^{48}$ reaction at 21° lab is shown in Fig. 6. The angular distributions of all groups show the typical behavior of $\ell = 3$ transitions. Transitions to the ground state and to the 2^+ and 4^+ states are observed. The transition to the group near 3.3 MeV excitation occurs at a Q value of -5.3 MeV while the ground-state Q value

---

[10] R. D. Lawson, Phys. Rev. 124, 1500 (1961).

[11] R. D. Lawson and B. Zeidman (to be published).

[12] L. H. Rietjens, O. M. Bilaniuk, and M. H. Macfarlane, Phys. Rev. 120, 527 (1960).

[13] J. F. Vervier, Nuclear Phys. 26, 10 (1961); O. Hansen, Nuclear Phys. 251, 140 (1961).

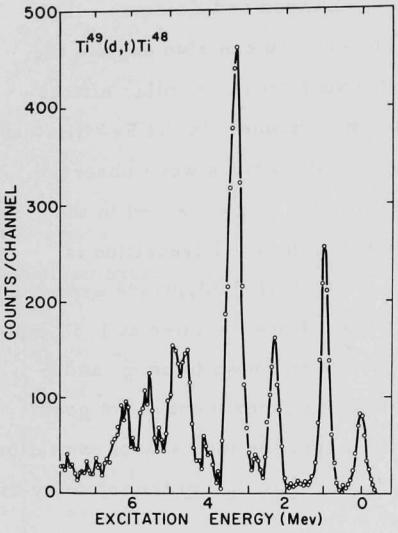

Fig. 6. The spectrum of $Ti^{49}(d,t)Ti^{48}$ at 21° lab. The spectrum has been corrected for the contributions from the Ti^{50} and Ti^{48} contained in the Ti^{49} target.

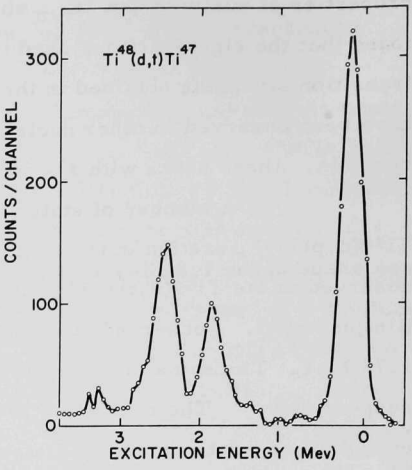

Fig. 7. The spectrum of $Ti^{48}(d,t)Ti^{47}$ at 21° lab.

for the Ti^{4} (d, t)Ti^{47} reaction is -5.36 MeV. While the 6^+ state in Ti^{48} has been found at 3.34 MeV,[14] it is not at all clear that the 3.3-MeV group involves transitions to this state only.

C. $Ti^{48}(d,t)Ti^{47}$

The spectrum obtained at 21° lab is shown in Fig. 7. The transition to the ground state of Ti^{47} is considerably weaker than the transition to the 160-keV level, if it is present at all. The ground-state spin of Ti^{47} is $\frac{5}{2}^-$ and if the neutron configuration of this state is $(f_{7/2})^{-3}$ one would not expect to observe the ground-state transition. The group leading to states near 2.4 MeV has an $\ell = 3$ angular distribution.

---

[14] K. Way et al., Nuclear Data Sheets, National Academy of Sciences, National Research Council, 1959 (U.S. Government Printing Office, Washington, D.C.).

Transitions to this state were not observed by Rietjens et al. in their $Ti^{48}(d, p)Ti^{47}$ experiment. However, an $\ell = 3$ transition in this energy region would have been completely masked by contributions from the $Ti^{48}(d, p)Ti^{49}$ reaction. The peak near 1.8 MeV shows a shoulder near 1.6 MeV. In the $Ti^{48}(d, p)Ti^{47}$ reaction, strong $\ell = 1$ groups were observed to states at 1.56 and 1.80 MeV. In the present experiment the peak shape of the 1.8-MeV group changes with angle. Therefore various portions of the peaks were analyzed separately. The resulting angular distributions are shown in Fig. 8. Curves a and b involve the low-energy end of the 1.8-MeV group and show the typical $\ell = 1$ behavior. Curves c and d are the curves derived from the high-energy end of the spectrum, while curve e is part of the 2.4-MeV group. Curves f

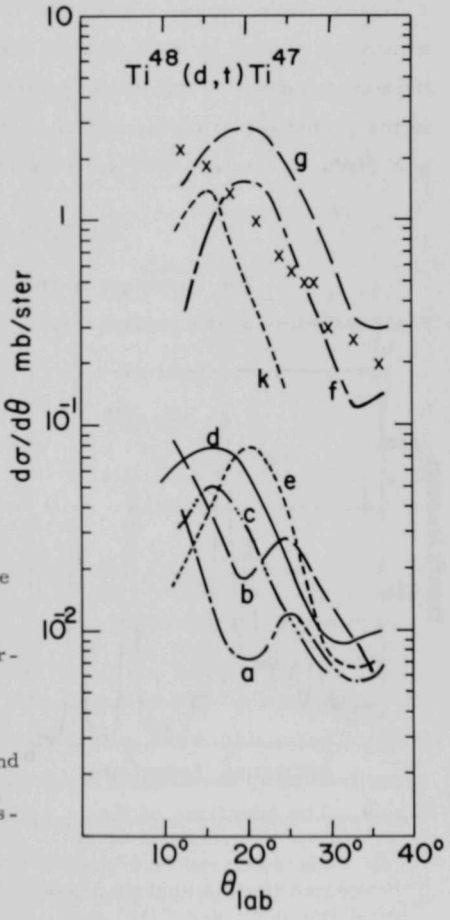

Fig. 8. Angular distributions for the $Ti^{48}(d, t)Ti^{47}$ reaction. Curves f and g are the angular distributions (in the laboratory system) of the transitions to the 0.16- and 2.4-MeV states of Ti^{47}. The crosses represent the angular distribution of the 1.8-MeV group. Curve a is the angular distribution from the portion from 1.5 to 1.6 MeV in the 1.8-MeV group, curve b is the portion from 1.6 to 1.7 MeV, curve c from 1.7 to 1.8 MeV, and curve d from 1.8 to about 1.9 MeV. Curve k is the angular distribution of the $Ca^{40}(d, t)Ca^{39}$ ground-state transition. Curve e is a section of the 2.4-MeV group.

and g are the angular distributions from the transitions to the 0.16- and 2.4-MeV groups, respectively. It is seen that these latter curves have similar angular distributions. This distribution is characteristic of $\ell = 3$ transitions in this region. Curves c and d are definitely different. In order to establish the angular distribution for $\ell = 2$, the $Ca^{40}(d, t)Ca^{39}$ ground-state reaction was used. It is shown in curve k. From this it follows that the transition to about 1.6 MeV is $\ell = 1$ and the one to the 1.8-MeV state has an $\ell = 2$ angular distribution. It is clear that a weak admixture of $\ell = 1$ in the 1.8-MeV state cannot be excluded on the basis of the present data. From the experimental data the admixture of 2p neutrons in the ground-state configuration of Ti^{48} is estimated to be approximately half of the 2p neutron admixture in Ti^{50}.

D. $Ti^{47}(d, t)Ti^{46}$

The spectrum is shown in Fig. 9. As is to be expected from the spins of the ground states, there is no evidence for the ground-state transition. The transitions to the 2^+ and the 4^+ states of Ti^{46} are quite strong. The transition to the 2.96-MeV state is, however, very weak if present at all. The determination of the cross section of the transition to this state is made difficult by the $Ti^{48}(d, t)Ti^{47}$ transition to the 160-keV state. Subtraction of the Ti^{48} contribution virtually eliminates the 2.96-MeV contribution. A strong group is observed with an excitation energy of about 3.9 MeV. The Q value for this group is approximately -6.5 MeV, while

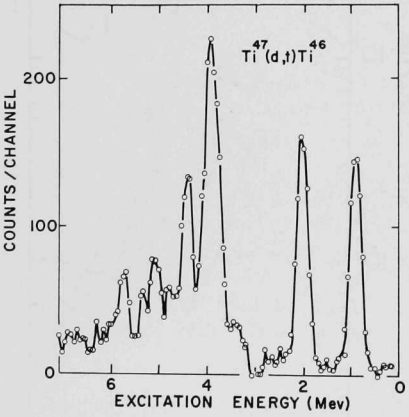

Fig. 9. The spectrum of the $Ti^{47}(d, t)Ti^{46}$ reaction at 21° lab. The spectrum has been corrected for the contributions from the Ti^{46} and Ti^{48} contained in the Ti^{47} target.

the Q value for the ground-state transition of $Ti^{48}(d, t)Ti^{45}$ is -6.9 MeV. It appears to be a general rule in this region of the periodic table that the (d, t) group with the largest cross section from targets with odd neutron number has a Q value a few hundred kilovolts higher than the Q value for the ground-state transition of the final even-even nucleus.

E. $Ti^{46}(d, t)Ti^{45}$

The spectrum at 21° lab is shown in Fig. 10. Here again there are two strong $\ell = 3$ transitions separated by about 2 MeV. The group near 3 MeV excitation could be due to Ca contamination. From the angular distribution, however, it appears that this is an $\ell = 3$ transition and that it should therefore be assigned to Ti^{46}. There is a possibility that an $\ell = 2$ admixture is present in the transition to a state at about 300 keV excitation. No groups with an $\ell = 1$ angular distribution have been observed.

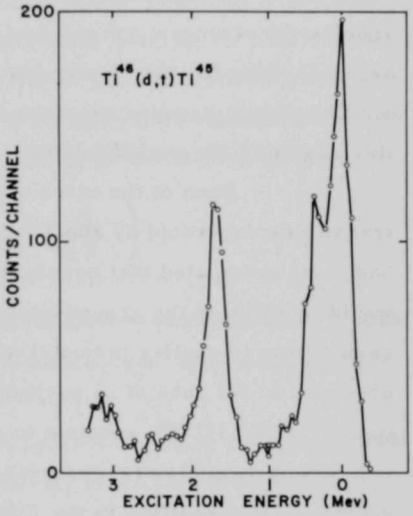

Fig. 10. The spectrum of the $Ti^{46}(d, t)Ti^{45}$ reaction at 21° lab. The spectrum has been corrected for the contributions from the Ti^{47} and Ti^{48} contained in the Ti^{46} target.

IV. CONCLUSIONS

Previous experiments on targets in the 1f-2p shell have been interpreted mainly through the use of sum rules in order to obtain information on the neutron configuration of the ground states. In the present experiment one may expect that a more detailed interpretation will be feasible. There are some noticeable similarities in the results on the titanium isotopes of odd mass.

Both show the expected large number of peaks. On the assumption that the 2.96-MeV state in Ti^{46} is the 6^+ state, it is apparent that the transition probabilities to the 2^+, 4^+, and 6^+ states in Ti^{46} are very different from those in Ti^{48} — at least if the strong peak near 3.4 MeV in Ti^{48} were to be identified with the 6^+ state at 3.34 MeV. Some difference in the ratios might be expected because of the ground-state spin of Ti^{47}. It appears more likely that the strong peak in Ti^{48} is due to more than one state, the 6^+ state making only a relatively small contribution. In both spectra the strongest group has a Q value which is approximately the same as the Q value for the ground-state (d, t) reaction on the final nucleus. Similar strong groups have been observed in other odd-neutron targets in this region of the periodic table.

Each of the three even-even targets showed two strong $\ell = 3$ transitions separated by about 2 MeV. In the case of Ti^{46} and Ti^{50} it had been anticipated that nearly the entire strength of the $f_{7/2}$ pickup would be found in the ground-state transitions. While core excitation had been observed earlier in nuclei with 28 and 30 protons, it had not been observed in the case of 26 particles. Since an $\ell = 2$ transition is observed in the Ti^{48}(d, t)Ti^{47} reaction to a fairly low-lying state and since there is a strong suspicion for the presence of an $\ell = 2$ transition close to the ground-state transition in the Ti^{46}(d, t)Ti^{45} reaction, it is plausible that calculations assuming an inert core of Ca^{40} and an active $(1f_{7/2})^n$ configuration will yield only approximate agreement with the experimental results.

I-30-1 Calculation of Reduced Widths from Resonant Scattering of Protons by a Diffuse Potential (51210-01)

J. P. Schiffer

The optical-model code ABACUS[1] has been used on the IBM-704 computer to calculate the scattering of protons by a real well with a diffuse surface. By use of the Saxon-Woods shape with the accepted values of radius and diffuseness ($R = R_0 A^{1/3}$, where $R_0 = 1.25$ fermi; and $a = 0.55$ fermi) which were obtained from numerous elastic scattering experiments at higher energies, it was found that the scattering resonances were appreciably narrower than the single-particle estimates[2] calculated from the conventional R-matrix formalism which gives

$$\Gamma = \frac{2k}{A_l^2} \left(\frac{3}{2} \frac{\hbar^2}{M R} \right). \qquad (1)$$

These scattering resonances are then an improved estimate of the single-particle width and can be used to give values of θ_p^2, the fraction of the single-particle width of a level.

The calculation has been applied to obtain a reduced width of the $d_{5/2}$ resonance found in the scattering of protons from carbon at 1.75 MeV.[3] This resonance was found to have a width of 61 keV, which is 0.21 times the Wigner-Teichmann limit calculated from Eq. (1) for a

---

[1] The ABACUS optical-model code has been developed by Drs. E. Auerbach and C. Porter of the Brookhaven National Laboratory.

[2] T. Teichmann and E. P. Wigner, Phys. Rev. 87, 123 (1952).

[3] H. L. Jackson and A. Galonsky, Phys. Rev. 89, 371 (1952).

radius of $1.45(12^{1/3}+1)$ fermi.[4] In the diffuse-surface optical-model calculation, the well depth was adjusted so that the $d_{5/2}$ level would occur at various energies of the incident proton. This graph of Γ vs E_p is shown in Fig. 11. Interpolating at 1.75 MeV, one finds that the $d_{5/2}$ scattering resonance has a width of 57 keV. It therefore seems that $\theta_p^2 \approx 1$ for this state so that it has the full single-particle width. Thus it is a very good single-particle state, as is expected from the shell model.

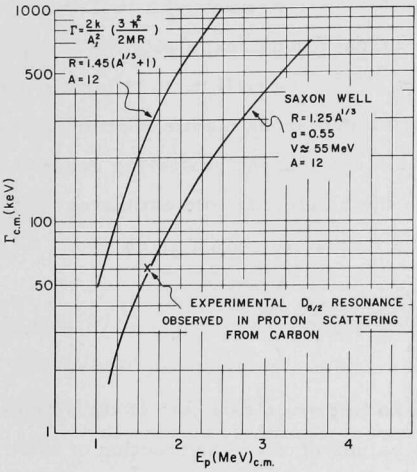

Fig. 11. Plot of the calculated width Γ of a $d_{5/2}$ proton single-particle state in C^{12} as a function of proton energy. The upper curve is from the R-matrix formalism, the lower one from a diffuse well. The cross indicates the experimental value found in reference 3.

Further calculations investigating the sensitivity of these widths to choice of radius and diffuseness are in progress. Reanalysis of elastic scattering resonances in some other nuclei is planned. It is always possible to choose a radius for which the width for the Wigner-Teichmann estimate will be the same as the one obtained from a diffuse potential. Preliminary trials indicate that this radius will be a function of energy, target nucleus, and angular momentum

---

[4] If one omits the $\frac{3}{2}$ in Eq. (1), as has been done by the original authors and in the compilation of A. M. Lane, Revs. Modern Phys. 32, 519 (1960), one gets $\theta_p^2 = 0.32$. The compilation of F. Ajzenberg-Selove and T. Lauritsen, Nuclear Phys. 11, 1 (1959), on the other hand, uses Eq. (1) with the factor of $\frac{3}{2}$ and gets the lower value of θ_p^2 mentioned in the text.

and that no simple corrections such as can be made for s-wave neutrons[5] seem likely. It is quite clear that the well-established diffuse surface of nuclei has a large effect on the magnitude of reduced widths obtained from proton widths of nuclear energy levels.

---

[5] E. Vogt (private communication).

I-98-29 Unbound Nuclear Energy Levels in the KeV Region (51210-01)

Carl T. Hibdon

NEUTRON BACKGROUND DUE TO Ta BACKINGS FOR LITHIUM TARGETS

The background due to neutron scattering from the tantalum backing for lithium targets has been measured at neutron energies from 2 to 300 keV for neutrons emitted at an angle of 120° with respect to the direction of the proton beam. The method consists in measuring the unfiltered neutron beam in this direction with and without a second piece of tantalum attached to the backing of the target and making the appropriate transmission corrections for the scattered neutrons. The second piece of tantalum used was an end cut out of another cap to ensure a snug fit as shown in Fig. 12. Without the second piece of tantalum A, I_0 neutron counts are registered. This count consists of two groups of neutrons: (1) the main group I_1 that

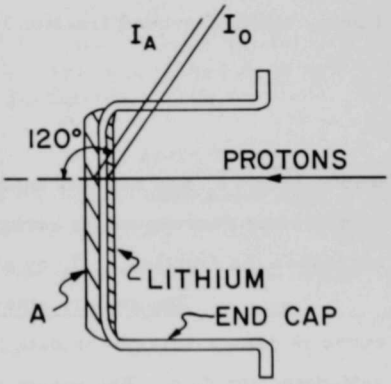

Fig. 12. Schematic cross section of the tantalum end-cap, showing the lithium layer inside. The tantalum layer A is of the same thickness (10 mils) as the end cap and is removable.

comes directly from the lithium layer on the inside of the tantalum end cap, and (2) a second group I_2 of higher energy neutrons that are scattered by the tantalum. A second set of measurements, with the extra piece of tantalum attached, produces I_A counts instead of I_0 because of the additional neutron scattering by the extra piece of tantalum. The additional counting rate $I_A - I_0$ is slightly less than I_2 because of a loss of neutrons in passing through the tantalum cap before being scattered by the second piece of tantalum A in Fig. 12 and in again traversing the cap after being scattered. The initial passage through the cap attenuates the neutron flux by the small factor $\exp(-N\sigma)$, where N and σ correspond to the 10-mil tantalum end cap. Subsequently, the scattered neutrons $(I_A - I_0)$ to the counter re-enter the tantalum end cap at an angle of 60° with the normal and hence suffer an additional attenuation of $\exp(-2N\sigma)$. Then, if multiple scattering is ignored, the total attenuation amounts to $\exp(-3N\sigma)$ and the background count is given by the expression

$$I_2 = (I_A - I_0) \exp(3N\sigma). \qquad (1)$$

Hence, the background fraction is given by

$$\frac{I_2}{I_0} = \left(\frac{I_A}{I_0} - 1 \right) \exp(3N\sigma), \qquad (2)$$

where I_0 and I_A are directly measurable quantities representing the net counts after corresponding backgrounds are subtracted. The factor $\exp(3N\sigma)$ increases the fraction I_2/I_0 by about 3-4% for a 10-mil tantalum end cap.

The results obtained are shown in Fig. 13, where the solid curve is drawn through the data for flat detection and the broken line through self-detection data. The insert shows the results for flat detection up to 25 keV on an expanded energy scale. Near 50 keV, the point shown by a cross was obtained by measurements near the peak of the resonance level of F^{20} at 49.7 keV. The point shown by a square gives the results obtained

by this method after corrections were made for the neutron energy spread.

One sees in Fig. 13 that the background fraction is large at low energies, but falls steeply with increasing neutron energy to about 6.5% at 10 keV. It subsequently decreases gradually to about 2.8% at 100 keV, where it begins to rise again and reaches a maximum of about 6.3% near 250 keV. The results are characterized by a low background fraction where the neutron yield is large, and larger fractions in regions of low neutron yield. Points for self-detection were obtained by setting the neutron energy at the peaks of known resonances in order to obtain large counting rates.

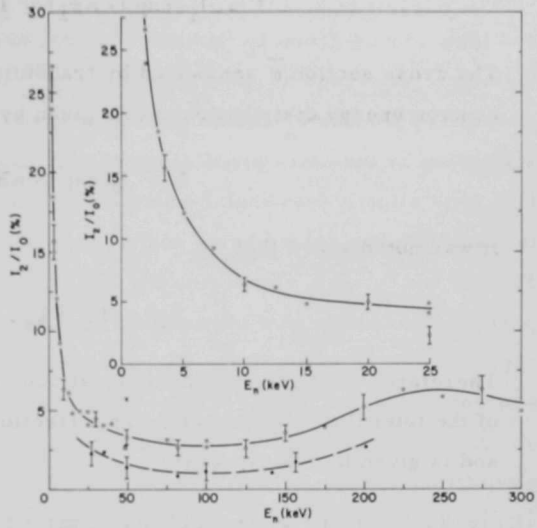

Fig. 13. The relative end-cap background I_2/I_0 from 2 to 300 keV neutron energy. The solid curve guides the eye for data obtained by flat detection and the dashed curve for the data obtained by self-detection. The insert shows the data obtained by flat detection from 2 to 25 keV on an expanded energy scale.

Once the background fraction has been measured, it can be used for corrections in the following way. Since the main group of neutrons I_1 from the lithium target correspond to a cross section σ_1 and the group of neutrons I_2 scattered by the tantalum correspond to a cross section σ_2, the transmitted beam I registered by the neutron counters for a transmission sample having n atoms per cm^2 is given by the expression

$$I = I_1 \exp(-n\sigma_1) + I_2 \exp(-n\sigma_2). \quad (3)$$

The cross section $\bar{\sigma}$ measured by transmission is the average over the neutron energy distribution and is given by

$$I = I_0 \exp(-n\bar{\sigma}). \quad (4)$$

It was noted above that

$$I_0 = I_1 + I_2. \quad (5)$$

Therefore, the background flux I_2 at 120° constitutes the fraction I_2/I_0 of the total flux at that angle. This fraction is obtainable from Eqs. (3-5) and is given by the expression[1]

$$I_2/I_0 = [1 - \exp n(\sigma_1 - \bar{\sigma})] / [1 - \exp n(\sigma_1 - \sigma_2)]. \quad (6)$$

A reasonable value of σ_2 can be estimated from cross section curves. By taking the measured value of the cross section to be $\bar{\sigma}$, the corrected value of σ_1 can be computed from the known value of I_2/I_0.

The most interesting consequence of the end-cap background is reflected in the observed value of $\bar{\sigma}$ near the peaks of narrow levels. At these positions, σ_2 usually (but not necessarily always) will be much less than σ_1 and a correction for the end-cap background will increase the observed value of $\bar{\sigma}$ as is shown in Table IV. This correction is in the right direction to aid in determining the peak heights of resonances, and hence their spins; but the magnitude of this correction normally is small in comparison with a correction for neutron energy spread.

Several special cases are worthy of mention. (1) If $\sigma_2 = \sigma_1$, Eqs. (3-5) show that $\bar{\sigma} = \sigma_1$. (2) If $\sigma_2 > \sigma_1$, as may some-

---

[1] H. W. Newson, E. G. Bilpuch, F. P. Karriker, L. W. Weston, J. R. Patterson, and C. D. Bowman, Ann. Phys. 14, 365 (1961).

TABLE IV. Some typical corrections obtained from Eq. (6) by use of end-cap background fractions from Fig. 13. The corrections are made for some narrow unbound levels of various peak heights in F^{20}. The quantity $\bar{\sigma}_0$ is the observed value of the cross section at the peak of a level and σ_c the corrected value.

	Flat-Detection				Self-Detection			
E_r (keV)	$\bar{\sigma}_0$ (barns)	n (10^{24} atoms/cm^2)	I_2/I_0 (%)	$\bar{\sigma}_c$ (barns)	$\bar{\sigma}_0$ (barns)	n (10^{24} atoms/cm^2)	I_2/I_0 (%)	$\bar{\sigma}_c$ (barns)
27.35	64.7	0.0151	4.4	68.0	88.8	0.00756	2.6	92.1
143.0	5.7	0.0779	3.2	5.0	6.1	0.0779	1.3	6.2
215.5	6.0	0.0779	5.7	6.15	6.55	0.0779	3.4	6.70
236.75	7.6	0.0457	6.2	7.9	8.65	0.0457	4.0	8.90
270.5	14.7	0.020	6.1	15.5	15.25	0.020	4.0	15.9

times occur in regions far away from resonances, $\bar{\sigma}$ will exceed σ_1 so the corrected value of $\bar{\sigma}$ will be less than the observed value. (3) If $\sigma_2 < \sigma_1$, then $\sigma_1 > \bar{\sigma}$. This is the case of main interest, discussed above. (4) For small peaks, $\bar{\sigma}$ and σ_1 will differ, but their values will usually be small. Therefore, the value of σ_1 calculated from Eq. (6) will depend on the values of σ_2 and N. This correction is small except when σ_2 is quite different from σ_1. For wide levels, $\bar{\sigma}$ differs little from σ_1 except in some special instances where σ_2 has unusual values. Hence the correction will be negligible. It should be noted that the observed value $\bar{\sigma}$ will be equal to the true value σ_1 near the peak of a resonance only if $\sigma_2 = \sigma_1$. This is true even for an isolated level unperturbed by interference from other levels or by contributions from their wings. However, for wide levels, the difference between $\bar{\sigma}$ and σ_1 may be negligible.

A full report on this topic is to be submitted for publication to Nuclear Instruments and Methods.

II. MASS SPECTROSCOPY

II-40-10 Fragmentation of Hydrocarbons (51300-01)

H. E. Stanton

In an earlier report,[1] two types of behavior of the yields of the various ionic fragments from a hydrocarbon under electron impact were described as the energy of the electrons was increased from about 200 eV to more than 2 keV. It was shown that the product of E and yield (where E is the electron energy) increased with the energy E — either increasing approximately linearly with ln E, or else leveling off to a constant value for the higher values of E. Since the two types of ions resulted from the original impact of an electron with a neutral molecule, a more detailed examination of the various modes of fragmentation seemed indicated. This required a determination of the possible reactions that intermediate ions and radicals would undergo, and an assessment of the probability of all the particular reactions involved in the formation of the ion that was finally detected.

According to a theory described by Rosenstock,[2] an ionic precursor A^+ will produce an ion B^+, i.e.,

$$A^+ \rightarrow B^+ + C, \qquad (1)$$

where C denotes the aggregate of all other particles (charged or uncharged) resulting from production of B^+ in the reaction, provided the

---

[1] H. E. Stanton and J. E. Monahan, Physics Division Summary Report ANL-6376, June 1961, p. 16.

[2] H. M. Rosenstock, Absolute Rate Theory for Isolated Systems and the Mass Spectra of Polyatomic Molecules, University of Utah, July 1952.

energy balance is favorable. Since both ions result from a single impact of an electron and the parent neutral molecule, enough energy must be transferred to the molecule to produce the ion A^+, i.e., the energy transferred must exceed the appearance potential $AP(A^+)$ for that ion. The electron must also supply the extra energy

$$\Delta H^f = AP(B^+) - AP(A^+) \tag{2}$$

in order to make reaction (1) possible.

If we consider a reaction

$$A \rightarrow B + C, \tag{3}$$

similar to Eq. (1) but involving only neutral particles, it will proceed as indicated provided the heat of formation $H_f(A)$ for A equals or exceeds the combined heats of formation plus any kinetic energy on the right-hand side of Eq. (3). If this is not so, the difference must be supplied. Values of some of these heats of formation are found in the literature,[3] but a complete listing does not appear to be available.

The heats of formation for Eq. (1) may be derived from Eq. (3) by adding the ionization potentials appropriate to the formation of the ion, i.e.,

$$H_f(A^+) = H_f(A) + IP(A^+), \tag{4}$$

where $IP(A^+)$ is the ionization potential for the ion A^+. Consequently, the heat of reaction for Eq. (1) is

$$\Delta H_f = H_f(B^+) - H_f(A^+) + H_f(C). \tag{5}$$

---

[3] Field and Franklin, Electron Impact Phenomena (Academic Press, Inc., New York, 1957).

The Rosenstock theory postulates, now, that

$$\Delta H^{\ddagger} \geq \Delta H_f; \tag{6}$$

but the assertion is that if

$$\Delta H^{\ddagger} \gg \Delta H_f$$

then the reaction is unlikely to occur. He argued that if the difference exceeded about 10 kcal/mole (0.4 eV) the probability was negligible.

In order to apply this theory to the five hydrocarbons measured in MA-17, a large number of appearance potentials, ionization potentials, and heats of formation were required. In many instances they were not available, apparently, but could be estimated from Eqs. (2), (4), and (5). This usually involved taking Eq. (6) as a true equation to calculate, for instance, the appearance potential for an ion. Such appearance potentials are known as "adiabatic" values since they tacitly assume all reacting components to be in the ground state, whereas measured values necessarily take account of products which are in excited states.

In many cases heats of formation were estimated from heats of combustion; and in still other cases, usually involving ionic properties, values were supplied by crude interpolations within the table itself. Fortunately, many of the more exotic values were for fragment species that did not enter into the reaction chains in an important way.

The thermochemical basis for understanding the Rosenstock theory is shown in Fig. 14, which is the energy diagram of the sample reactions

$$C_6H_6 \rightarrow C_6H_5^+ + H \rightarrow C_3H_3^+ + C_3H_2 + H \tag{7}$$

and

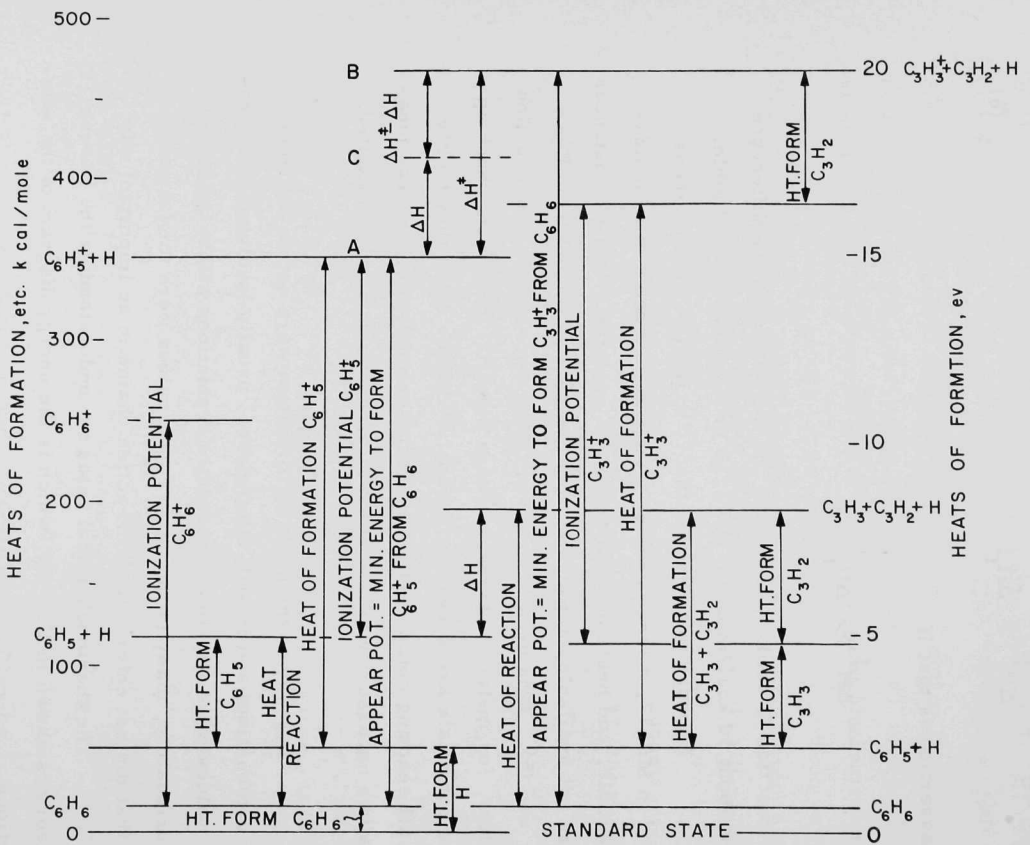

Fig. 14. The heats of formation for neutral and ionic species, ionization potentials, appearance potentials, and heats of reaction for the sample reactions of Eqs. (7) and (8)—shown in the form of an "energy level" diagram. The criterion of Rosenstock and its implications in Eq. (11) are shown near the center at the top of the diagram.

$$C_6H_6 \rightarrow C_3H_3^+ + C_3H_2 + H. \qquad (8)$$

Energetically, both sequences of reactions are possible for the production of ions of mass 39^+ from benzene.

The left-hand half of the diagram is for the first reaction in sequence (7). The various energy levels shown are for the formation of the intermediate radicals leading to the formation of $C_6H_5^+$. This assumes, of course, that everything is in the ground state, both electronically and vibrationally. On the right-hand side of the figure is the corresponding diagram for reaction (8), the direct formation of $C_3H_3^+$ from the parent molecule $C_6H_6^+$. Indicated levels below about 200 kcal/mole involve thermochemical reactions of neutral species only, whereas the ones above that value all involve ionization.

The second reaction in sequence (7) will take place provided

$$\Delta H^{\ddagger} \geq \Delta H_f, \qquad (9)$$

because of the following considerations. It is clear that the appearance potential for the formation of an ion from a neutral molecule must include the heat of reaction of the neutral particles, the ionization potential, and any energy of activation for the fragment in question. If the ion formed is to be a stable ion, there can be no competing reaction with a lower threshold, since then the first reaction would never take place. In the reaction

$$C_6H_5^+ \rightarrow C_3H_3^+ + C_3H_2, \qquad (10)$$

the ion $C_6H_5^+$ must have an additional amount of internal energy to supply the thermochemical heat of reaction ΔH. The level A at 334 kcal/mole represents the total energy necessary to form the ion $C_6H_5^+ + H$ in

the ground state from the standard states of its components. The total energy for an ion which can further react as in Eq. (10) is larger by the amount ΔH (as for level C in Fig. 14). It therefore follows that the energy extracted from the bombarding electron to create this highly excited ion must exceed the ground-state appearance potential by ΔH also. Since the threshold for the formation of $C_3H_3^+$ is its appearance potential, if reaction (10) is to be possible, Eq. (9) must hold. Otherwise reaction (8) would be controlling and the intermediate ion $C_6H_5^+$ would not appear in this sequence. In the figure, the level marked B must be at a higher energy than the one designated C. If this is not so, the reaction is impossible.

If Eq. (9) is now assumed to be true, the energy driving reaction (10) in the forward direction is given by

$$H = \Delta H^{\ddagger} - \Delta H_f . \tag{11}$$

If it is further assumed that classical theory applies, the rate constant is

$$k = Ae^{-H/kT} , \tag{12}$$

where A is a frequency factor, H is given by Eq. (11), k is Boltzmann's constant, and T is the temperature. In the following analysis of the fragment distributions, it was assumed that the frequency factor A was the same for all fragments from a given molecule, but varied for different molecules.

CALCULATIONS OF THE REACTIONS

A single saturated-hydrocarbon molecular species C_iH_{2i+2} can give rise to i(i+3) different kinds of daughter ions which are singly charged, if one considers only the successive extraction of individual atoms. Unsaturated compounds will give fewer succeeding ions, of course; but even for the simplest hydrocarbon there are seven distinct arrangements including the parent ion.

Since any ion, according to this limited approach, can produce any other ion with either fewer carbons or fewer hydrogens or both, the total number of reactions leading from one ion to another with fewer atoms will be $\frac{1}{2}\ [i(i+2)]^2$ — except for some corrections for counting the same reaction more than twice and for constraints introduced by the energetics of the reactions. Thus a digital computer was used to enumerate the possible reactions and to compute the corresponding values of ΔH_f, $\Delta H^{\ddagger}$, and their differences $\Delta H^{\ddagger} - \Delta H_f$.

There are further complications which introduce many more reactions. In reaction (1) it has been tacitly assumed that the fragments left over and denoted by C have a unique configuration. Such is not the case. Conservation of particles requires that the number of carbon atoms in B^+ and C should add up to the number of carbon atoms in A^+, etc. For different values of these numbers of atoms in A^+ and B^+, the atoms left over from the formation of B^+ may have a large number of possible configurations in from zero to several distinct fragments, each representing a separate disintegration reaction with its own set of energetics. These usually differ from those of an alternative mode, but give the same ionic product B^+.

In the actual calculation, it was assumed that only a single, singly-charged ion was formed in any reaction. It was further assumed that all remaining carbon atoms were aggregated into one neutral fragment, but with differing numbers of attached hydrogens. Any remaining hydrogens were assumed to form neutral fragments H_2, unless there was an odd number. This last assumption may differ from reactions postulated by other investigators in some instances.

Each hydrogen atom left as a free atom changes ΔH_f by 51 kcal/mole, whereas $\Delta H^{\ddagger}$ remains unchanged. Their difference is, therefore, greatly altered thereby, and the probability of the production of the ion by the reaction in question is changed by an order of magnitude.

Limits of from -5 kcal/mole to +50 kcal/mole were set for the quantity $\Delta H^{\ddagger} - \Delta H_f$. The small negative lower limit (which should be 0 theoretically) was necessary because several known reactions were eliminated without it. It may represent errors in the values found in the literature. For differences greater than 50 kcal/mole, it was assumed that the probability was so small that the reaction could be neglected.

Two other items were noted when the results of these calculations were compared with known distributions of fragments. Although Rosenstock indicated that a reaction was practically unable to proceed if $\Delta H^{\ddagger} - \Delta H_f \gtrsim$ 10-15 kcal/mole, it was discovered that such a small upper limit again eliminated the production of some ions that were known to exist.

The second item was concerned with the production of saturated products. As nearly as could be determined, no secondary reaction occurred, even though energetically favorable, if it produced a saturated hydrocarbon as either the neutral fragment C or the ionic product B^+ in reaction (1). That is, neither of the reactions

$$C_2H_4^+ \rightarrow C^+ + CH_4$$

$$C_2H_4^+ \rightarrow CH_4^+ + C$$

proceeded, even though they may have been permitted by the energetics. This is a rather bizarre example because of rather obvious geometric objections, but for other molecules this objection does not apply. For instance, geometric hindrance is not sufficient to prevent the formation of CH_3^+ from benzene, and one would suppose there would be no important hindrance to the formation of CH_4 from neopentane or C_2H_6 from normal heptane. In some instances, well known and reliable measurements

indicate that such reactions are energetically quite favored; but still their complete elimination improves the agreement with the experimental fragmentation patterns.

CALCULATION OF THE YIELDS

Let

$$H_{ij} = \Delta H_{ij}^{\ddagger} - \Delta H_{f,ij} \tag{13}$$

for the reaction that produces the jth ion from the ith ion as precursor. If N_i is the concentration of the ith ion, and a_{ik} is proportional to the probability that it is formed from the kth ion, then in the reaction volume the rate of change of concentration of the ith ion is

$$\frac{dN_i}{dt} = \sum_{k=1}^{i-1} a_{ik} N_k - N_i \sum_{j=i+1}^{m} a_{ji} - a_1 N_i, \tag{14}$$

where a_{ji} is proportional to the probability that the ith ion will spontaneously break up to form the jth ion, a_1 is proportional to the probability that it will leave the reaction zone intact, and m is a suitable upper limit representing the smallest ion obtainable.

In a mass spectrometer, the time spent in the ion box by such an ion may approach 10^{-5} sec whereas the time for fragment formation is of the order of 10^{-8} sec. It, therefore, seems appropriate to assume that the concentrations of the various fragments are given by the set of equations

$$\sum_{k=1}^{i-1} a_{ik} N_k - N_i \left(a_1 + \sum_{i=j+1}^{m} a_{ji}\right) = 0, \tag{15}$$

obtained from Eqs. (14) by equating the derivatives to zero. It is pre-

sumed that the response of the mass spectrometer is proportional to the N_i.

The ion intensities Y_i are determined from the measurements, and it is proposed to determine the relationship between the a_{ik} and the $\Delta H_{ik}^{\ddagger}$ such that the N_i agree as well as possible with the Y_i.

The results of mass spectrometric measurements are not ordinarily given in absolute units but are normalized to one of the fragment yields, usually the parent ion. One, therefore, is led to assume that

$$N_1 = \text{constant} \tag{16}$$

although some other ion may be taken as the standard. For convenience, the Y_i are also relative, and if the yields are normalized to that of the parent ion, then

$$Y_1 = 1 \qquad \text{and} \qquad N_1 = 1. \tag{17}$$

For purposes of reducing the existing data, the general relation proposed for a_{ji} is

$$a_{ji} = e^{-a_2 H_{ji}}. \tag{18}$$

This brings the number of independent parameters to two: a_1 and a_2. Two criteria are needed. The two additional restrictions that have been assumed are

$$\sum_{i=1}^{m} (N_i - Y_i) = 0 \qquad \text{and} \qquad \sum_{i=1}^{m} (N_i - Y_i)^2 = \text{minimum}. \tag{19}$$

There also are the physical limitations that

$$a_1, a_2 > 0. \tag{20}$$

The results of the calculations are shown in Figs. 15-17.

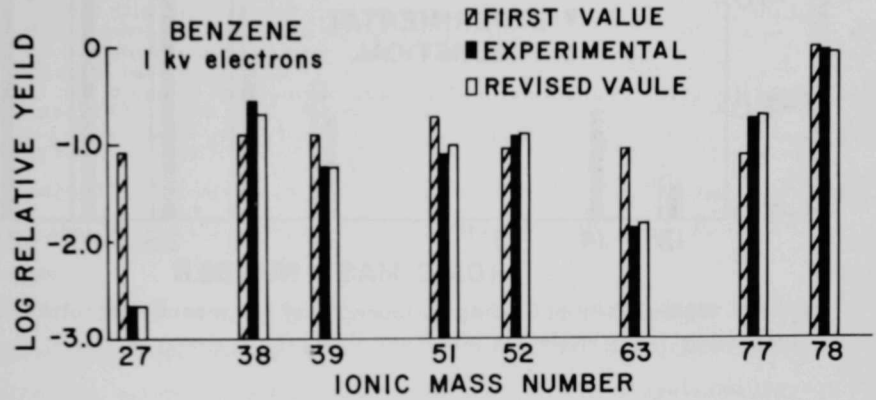

Fig. 15. The mass spectrum for benzene, C_6H_6, as measured for 1000-eV electron impact (solid bars), compared with two computed spectra. The shaded bars show the spectrum computed from Eqs. (15) and (18) by use of initial values of heats of formation etc. as found in the literature. The open bars represent the computed values when the H_{ji} of Eq. (13) were changed somewhat to give a better empirical fit.

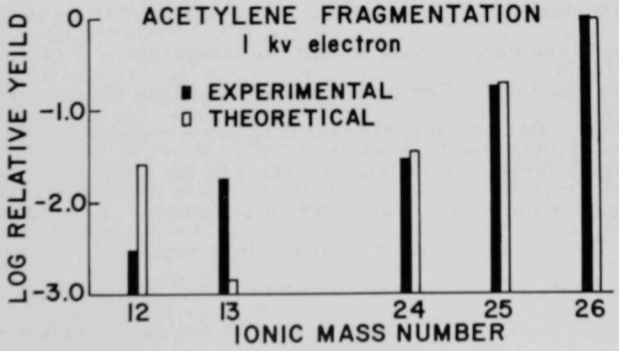

Fig. 16. Comparison of the calculated (open bars) and measured (solid bars) mass spectrum for acetylene, C_2H_2, under bombardment by electrons of 1000-eV energy. The H_{ji} were the original values tried.

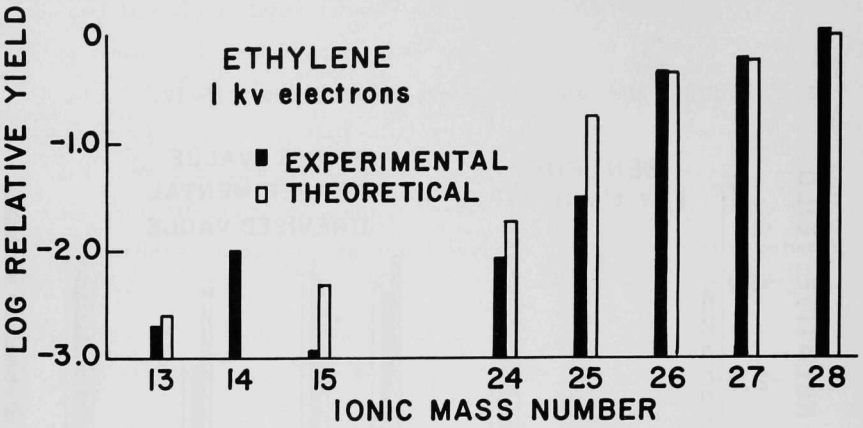

Fig. 17. Comparison of calculated (open bars) and measured (solid bars) mass spectra the molecule ethylene, C_2H_4.

RESULTS AND DISCUSSION

The use of the exponential form in Eq. (12) for unimolecular reactions of the class under consideration is a simplifying assumption, as is the uniformity of the value of a_2 for the fragments of a given molecule. In the classical theory, the reactants are assumed to be in thermal equilibrium with the environment so that the temperature T is the temperature of the surroundings. For unimolecular reactions the interpretation of T is nebulous. One can suppose that it is some measure of the total internal energy (vibrational, rotational, etc.) in the precursor, but this energy probably does not have a Maxwellian distribution. Alternatively, one can assume T to be the temperature that a bath must have in order that an ion with this same internal energy would be in equilibrium with it. There has been extensive theoretical investigation of the rate constant k for unimolecular reactions, none of the theories giving the exponential form assumed in Eq. (12). However, because of its suitability and analytical simplicity, it was used in reducing the data.

Figure 15 compares the experimental yields with two sets of theoretical yields for the fragmentation of benzene. The values of H_{ji} which determine the rate constant for the ith ion reacting to give the jth ion (as derived from the values of heats of formation, etc., given in the literature) gave the computed values shown by the shaded bars in Fig. 15 for the eight largest peaks. The second set of values (solid bars) was computed with values of H_{ji} derived from the first set by arbitrarily adjusting them to give a better empirical fit. The method selected for this arbitrary adjustment was to alter the appearance potential of a particular ion, and was as arbitrary as the amounts by which these values were changed.

Relative to the appearance potentials themselves (a few hundred kcal/mole) the changes were, generally, quite small ($<$ 10-20 kcal/mole), however. Referring again to Fig. 15, the largest change (26 kcal/mole) was made for the ion of mass 63 from benzene, which has an appearance potential of 382 kcal/mole. A change of 4 kcal/mole was introduced to correct the yield at mass 52, for which the appearance potential is 364 kcal/mole.

One can assume that these changes are required as a result of errors in measurement of the yields, in published or derived values of the various heats of reactions, in the appearance potentials, or a combination of these. One notes from Eqs. (5) and (13) and from the discussion above that the H_{ji} depend upon four energies, and are the difference of differences of these quantities. It is not surprising, therefore, that errors in determination of these heats could accumulate in such a way that some of the H_{ji} could be substantially in error. The example above of a change of 26 kcal/mole could quite possibly be spread among all four quantities to give an error of $\sim$7 kcal ($< \frac{1}{5}$ eV) in each.

The mass spectra of fragments from the other molecules studied could be similarly fitted by judicious adjustment of the H_{ji} within the same limits as for benzene. These are shown in Figs. 16 and 17.

The theory used in this analysis was an extension of the theory proposed by Rosenstock, augmented by classical reaction-rate theory, and adapted to a computer. It seems essentially to be an application of simple principles of energy conservation, with the relation in Eq. (12) introduced on an empirical basis. (Other simpler forms were tried and discarded.) Consequently, the basis of the yield calculations may have doubtful theoretical foundations.

This quasi-empirical "curve fitting" procedure may, however, have application to electron-impact phenomena. If this technique is found to have wider application, it may serve as a useful tool in interpreting a molecular fragmentation pattern to deduce the various quantities involved in a particular reaction. It may permit the calculation of the appearance potentials for unusual ions produced from other ions, for instance, if the appearance potentials of the latter are well known. If the appearance potential of an unusual ion is measurable, its heats of formation may conceivably be computed by the judicious use of the mathematical relationships.

According to the equilibrium theory of reaction rates, the coefficient a_2 in the analysis is equal to $1/kT$. If kT at room temperature is 0.5 kcal/mole, a_2 should have a value 2 for reactions that take place at that temperature. However, the earlier assumption that T was related to the internal motion of the precursor ion would imply that values of kT much larger than 0.5 kcal/mole would be reasonable. Again, in the case of benzene, $kT \approx 2.5$ kcal/mole, i.e., $T \approx 1500^{\circ}K$. This does not seem to be an unreasonably high value, since the constant a_2 represents a sort of average for most of the fragmentation reactions of the molecule, and since the lifetimes of the reacting ions (measured in microseconds) imply high internal energy.

Values of a_1 and a_2, and T for the other molecules analyzed are set forth in Table V.

TABLE V. The values of a_1 and a_2 as defined in Eqs. (15) and (18) and computed by a least-squares adjustment to give a "best fit" to the measured mass spectrum. The temperature T, derived from a_2 by use of Eqs. (12) and (18), is also included. The constant a_1 depends on the experimental arrangements and does not appear to be of fundamental significance.

Molecule	a_1 (sec^{-1})	a_2 $(kcal/mole)^{-1}$	T (^oK)
C_2H_2	1.769	1.105	543
C_2H_4	0.477	0.332	1810
	0.517	0.315	1900
	(0.800)	(0.241)	(2490)
C_7H_{16}	0.399	0.721	830
	0.404	0.716	842
	(0.391)	(0.616)	(973)
C_6H_6	4.01	0.464	1293
	(5.27)	(0.499)	(1200)

Theoretical studies of the rate constant and fragmentation of hydrocarbons are being continued in the hope of finding a more reliable theoretical foundation.

V. THEORETICAL PHYSICS, GENERAL

V-45-19 Meson-Nucleon Interaction (51151-01)

K. Tanaka

In the hypothesis of generalized isospin independence (GII),[1] the contribution of common channels to various two-particle states (whose total cross sections are considered) is assumed to be equal at sufficiently high energy. The particles are expected to become insensitive to their intrinsic properties at high energy so long as the conservation laws are respected. Then it is meaningful to discuss the inequalities between total cross sections in terms of the available noncommon channels which are possible under the conservation laws. Various differences of total cross section were written down on this basis. The number of possible final states (noncommon channels) was found to be larger when the states had smaller intrinsic quantum numbers (baryon number B, strangeness S, and isospin I_3).

In order to find the Regge poles[2] that appear in the crossed channel, a description of the KN system that can also be used for the NN system and whose crossing relations are transparent is presented.

The results are summarized in Table VI. The contribution of each Regge pole is designated by its letter. For π-N scattering, the corresponding contributions of Regge poles to the differences of total cross sections can be obtained by charge independence from

---

[1] K. Hiida, M. Soga, and K. Tanaka, Phys. Rev. Letters 8, 187 (1962).

[2] G. F. Chew and S. C. Frautschi, Phys. Rev. Letters 7, 394 (1961); 8, 41 (1962); B. M. Udgaonkar, Phys. Rev. Letters 8, 142 (1962).

TABLE VI. Comparison of differences of total cross sections.

Cross sections	Regge pole	GII	Experiment
$\sigma(K^+p) - \sigma(K^+n)$	$-\rho$	$= 0$	≈ 0 [a]
$\sigma(K^-p) - \sigma(K^-n)$	ρ	> 0	> 0 [b]
$\sigma(K^-p) - \sigma(K^+p)$	$\omega + \rho$	> 0	> 0 [c]
$\sigma(K^-n) - \sigma(K^+n)$	$\omega - \rho$	> 0	
$\sigma(pp) - \sigma(pn)$	$\pi - \rho'$	$= 0$	≈ 0 [d]
$\sigma(\bar{p}p) - \sigma(\bar{p}n)$	$\pi + \rho'$	> 0	
$\sigma(\bar{p}p) - \sigma(pp)$	$\omega' + \rho'$	> 0	> 0 [e]
$\sigma(\bar{p}n) - \sigma(pn)$	$\omega' - \rho'$	> 0	

[a] V. Cook, D. Keefe, L. T. Kerth, P. G. Murphy, W. A. Wenzel, and T. F. Zipf, Phys. Rev. Letters 7, 182 (1961). One may obtain some hints of the behavior of differences of total cross sections at high energies from data around 2 - 4 BeV.

[b] V. Cook, Bruce Cork, T. F. Hoang, D. Keefe, L. T. Kerth, W. A. Wenzel, and T. F. Zipf, Phys. Rev. 123, 320 (1961).

[c] G. von Dardel, D. H. Frisch, R. Mermod, R. H. Milburn, P. A. Piroué, M. V. Vivargent, G. Weber, and K. Winter, Phys. Rev. Letters 5, 333 (1960); E. W. Jenkins, W. F. Baker, R. L. Cool, T. F. Kycia, R. H. Phillips, and A. L. Read, Bull. Am. Phys. Soc. 24, 433 (1961).

[d] A. Ashmore, G. Cocconi, A. N. Diddens, and A. M. Wetherall, Phys. Rev. Letters 5, 576 (1960).

[e] G. von Dardel, D. H. Frisch, R. Mermod, R. H. Milburn, P. A. Piroué, M. V. Vivargent, G. Weber, and K. Winter, Phys. Rev. Letters 5, 333 (1960); M. J. Longo, J. A. Helland, W. N. Hess, B. J. Moyer, and V. Perez-Mendez, Phys. Rev. Letters 3, 568 (1959); R. Armenteros, C. A. Coombes, B. Cook, G. R. Lambertson, and W. A. Wenzel, Phys. Rev. 119, 2068 (1960); S. J. Lindenbaum, W. A. Love, J. A. Niederer, S. Ozaki, J. J. Russell, and L. C. L. Yuan, Phys. Rev. Letters 7, 185 (1961).

the relation $\sigma(\pi^- p) - \sigma(\pi^+ p) = \rho$. This interpretation and the GII interpretation are in agreement.

In the absence of detailed experimental information on the energy dependence of various combinations of total cross sections, the comparison of differences of total cross sections would give information on the validity of these possible interpretations. It appears to be important to see whether or not the present trend of the total cross section (Table VI) persists at higher energies.

V-47-1 Structure of Elementary Particles (51151-01)

K. Hiida

CHARGE STRUCTURE OF THE NUCLEON

We shall first summarize three useful theorems obtained from meson theory, which hold for the electromagnetic form factors of the nucleon.

Theorem I: The total charge contributed from three-pion intermediate states is zero, even under the influence of strong pion-pion interactions.

Theorem II: The Fourier transform of $F_{1n}(q^2)$ has a negative value, at least in the outermost region.

Theorem III: The proton has a charge $Z_{2p}e$ at its origin, where Z_{2p} is the bare-state probability of the proton and satisfies the relation

$$1 > Z_{2p} \geq 0 .$$

On the other hand, the neutron cannot have any charge at its origin.

Using these theorems and more detailed information from pseudoscalar meson theory leads to the following. If we omit the contribution from three-pion intermediate states, there is the isoscalar charge $\frac{1}{2}e$ near the origin of the nucleon. The role of the three-pion intermediate states is to polarize the vacuum. In other words, in the analogy with quantum electrodynamics it appears that the positive charge $\frac{1}{2}e$ near the center of the nucleon attracts the negative charge $-\delta e \equiv -a_\omega e$ and repels the positive charge δe. The role of the three-pion resonance ω is to enhance the polarization very strongly. For a long time the smallness of the rms radius of the neutron was a mystery. Nowadays the mechanism to reduce the radius is clear. Because of the strong vacuum polarization due to ω, the positive charge $a_\omega e$ moves far away from the center of the nucleon and hence $\langle r^2 \rangle_{1s} \approx \langle r^2 \rangle_{1v}$; that is, $\langle r^2 \rangle_{1n} \approx 0$.

One may ask whether the bare proton is surrounded by positive charge alone or by both positive and negative layers of charge. According to theorem III, the proton has the charge $Z_{2p}e$ at its center. This bare charge is concealed by the clouds contributed from massive intermediate states, and the negative charge cloud caused by the vacuum polarization due to ω. Since the vacuum polarization is very strong, the bare charge should be concealed by the negative charge cloud. Further, this layer of negative charge is surrounded by a layer of positive charge. Our proton model is represented schematically in Fig. 18(a).

The author would like to stress here a method to confirm this proton model, namely, that it is sufficient to show experimentally that there exists such a q^2 that

$$F_{1p}(q^2) < -\frac{1}{3},$$

where the number three comes from the fact that we live in three-dimensional space. The 2-mile machine at Stanford may be able to confirm the existence of such a value of q^2.

The neutron has no bare charge at the origin. In the innermost region, there is a negative charge, mainly due to the vacuum polarization. The middle region is occupied by positive charge because the vacuum polarization is so strong that the resulting positive charge is greater than the negative charge caused by $\rho\,(a_\omega > a_\rho)$. The outer region is occupied by negative charge. It is easy to show that F_{1n} has a negative sign for small values of q^2. Our neutron model is represented schematically in Fig. 18(b).

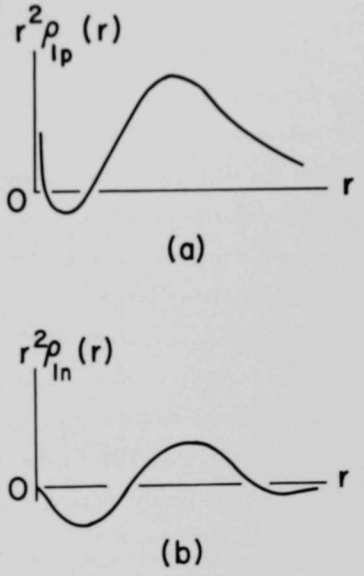

Fig. 18. Schematic representation (a) of our proton model and (b) of our neutron model — both in arbitrary scale.

PUBLICATIONS SINCE THE LAST REPORT

PAPERS

EXPERIMENTAL ANALOG STUDY OF CONTAINMENT OF DENSE PLASMAS IN RESONANT-CAVITY FIELDS
A. J. Hatch and J. W. Butler . . . . . .(Project IV-10)
J. Electronics and Control 12, 89-103 (February 1962)

NUCLEAR MODELS, THRESHOLD STATES AND REARRANGEMENT ENERGY
D. R. Inglis . . . . . (Project V-3)
Nuclear Phys. 30, 1-29 (1962)

GEOMETRICAL CONSIDERATIONS IN THE MEASUREMENT OF THE RATIO L/R IN THE SCATTERING OF POLARIZED NUCLEONS
J. E. Monahan and A. J. Elwyn . . . . . .(Project I-18)
Nuclear Instr. and Methods 14, 348-350 (January 1962)

FLUX QUANTIZATION AND THE CURRENT-CARRYING STATE IN A SUPERCONDUCTING CYLINDER
H. J. Lipkin, M. Peshkin, and L. J. Tassie . . .(Project V-33)
Phys. Rev. 126, 116-117 (April 1, 1962)

THE PION-PION EFFECT ON LOW-ENERGY PION-NUCLEON SCATTERING
M. Marinaro and K. Tanaka . . . . . .(Project V-45)
Nuovo cimento 23, 537-546 (February 1, 1962)

FLUORESCENCE ENERGY TRANSFER AND OXYGEN QUENCHING IN SOLUTIONS OF DIPHENYLOXAZOLE IN CYCLOHEXANE
A. Weinreb . . . . . (Project I-144)
J. Chem. Phys. 36, 890-894 (February 15, 1962)

ABSTRACTS

Washington meeting of the American Physical Society, April 23-26, 1962.

(d,He^3) REACTIONS ON F^{19} AND Al^{27}
T. H. Braid and B. Zeidman . . . . . (Project I-22)
Bull. Am. Phys. Soc. 7, 300 (April 23, 1962)

Washington meeting of the American Physical Society (cont'd.)

MOSSBAUER EFFECT OF Fe^{57} AS AN IMPURITY IN VARIOUS ALLOYS
J. Heberle, P. Parks, and J. P. Schiffer . . . .(Project I-19)
Bull. Am. Phys. Soc. 7, 350 (April 23, 1962)

DIRECT OBSERVATION OF RESONANT p-WAVE NEUTRON CAPTURE
H. E. Jackson . . . . . .(Project I-7)
Bull. Am. Phys. Soc. 7, 289 (April 23, 1962)

SPUTTERING EXPERIMENTS IN THE RUTHERFORD COLLISION REGION
M. S. Kaminsky . . . . . .(Project II-23)
Bull. Am. Phys. Soc. 7, 346 (April 23, 1962)

POLARIZATION AND DIFFERENTIAL CROSS SECTION FOR NEUTRONS SCATTERED FROM DEUTERIUM
R. O. Lane, A. J. Elwyn, and A. Langsdorf, Jr. . .(Project I-18)
Bull. Am. Phys. Soc. 7, 333 (April 23, 1962)

$Sm^{149}(n,\gamma)Sm^{150}$ AND THE ASSOCIATED ENERGY LEVELS IN Sm^{150}
R. K. Smither . . . . . .(Project I-60)
Bull. Am. Phys. Soc. 7, 316-317 (April 23, 1962)

(d,t) REACTIONS ON NUCLEI NEAR N = 28
B. Zeidman and T. H. Braid . . . . . (Project I-22)
Bull. Am. Phys. Soc. 7, 315 (April 23, 1962)

ANL TOPICAL REPORT

THE MEASUREMENT OF ENERGY AND INTENSITY OF GAMMA RAYS BY USE OF A SCINTILLATION SPECTROMETER . . . .(Project I-55)
R. T. Julke, J. E. Monahan, S. Raboy, and C. C. Trail
Argonne National Laboratory Topical Report ANL-6499 (April 1962)

CO-OP STUDENT REPORT

TECHNIQUE OF CORRECTING FOR NEUTRON-DETECTOR EFFICIENCY
D. J. Mueller . . . . . (Project I-18)
Co-op Student Report to Northwestern University, March 1962

ADDITIONAL PAPERS ACCEPTED FOR PUBLICATION

ELASTIC AND INELASTIC SCATTERING OF 43-MEV ALPHA PARTICLES BY Ni^{58} AND Ni^{60} . . . . . (Project I-22)
H. W. Broek, T. H. Braid, J. L. Yntema, and B. Zeidman
Phys. Rev. (May 15, 1962)

HEAVY-PARTICLE STRIPPING AND THE STRUCTURE OF Li^6
D. R. Inglis . . . . . (Project V-3)
Phys. Rev. (June 1, 1962)

RESONANT ABSORPTION OF NEUTRONS BY CRYSTALS
H. E. Jackson and J. E. Lynn . . . . . (Project I-7)
Phys. Rev.

SPUTTERING EXPERIMENTS IN THE RUTHERFORD COLLISION REGION
M. S. Kaminsky . . . . . (Project II-23)
Phys. Rev. (May 1962)

(d,t) REACTION STUDIES ON IRON AND NICKEL . . . . (Project I-22)
M. H. Macfarlane, B. J. Raz, J. L. Yntema, and B. Zeidman
Phys. Rev. (July 1, 1962)

HIGH-ENERGY GAMMA RAYS FROM Na^{24}
J. E. Monahan, S. Raboy, and C. C. Trail . . . (Project I-55)
Nuclear Phys. (June 1962)

ON THE FLUORESCENCE SPECTRUM AND DECAY TIME OF NAPHTHALENE
A. Weinreb and I. B. Berlman (RPY) . . . . . (Project I-144)
Molecular Phys.

THE ARGONNE 60-IN. SCATTERING CHAMBER
J. L. Yntema and H. W. Ostrander (CS) . . . . . (Project I-22)
Nuclear Instr. and Methods (July 1962)

PERSONNEL CHANGES IN THE ANL PHYSICS DIVISION

NEW MEMBERS OF THE DIVISION

Technician

Mr. John D. Oyler joined the Physics Division on April 11, 1962, as a Research Technician Jr. under the supervision of G. J. Perlow.

DEPARTURE

Dr. Sippanondha Ketudat, Institute Affiliate, has been in the Argonne Physics Division since November 4, 1960. He worked with M. T. Burgy and G. R. Ringo on cobalt mirrors to polarize neutrons (Project I-123) and with S. Raboy and C. C. Trail on the conservation of parity in strong interactions (Project I-55). He left ANL on April 13, 1962 to return to the Department of Physics, Chulalongkorn University, Bangkok, Thailand.